

## THEORETICAL TEMPERATURE-DEPENDENT PHONON SPECTRA OF SOLID NEON

T. R. Koehler

IBM Research Laboratory, San Jose, California 95114

(Received 11 February 1969)

Recent measurements of the temperature dependence of phonon energies in solid neon do not agree with the results of previous theoretical treatments. This discrepancy is remedied here with a calculation of the one-phonon Green's function by a perturbative method which includes the leading corrections to the lowest order self-consistent phonon theory. The renormalized phonon energy is then identified with the peak of the imaginary part of the Green's function.

Recent inelastic neutron-scattering measurements in solid neon<sup>1</sup> have uncovered an interesting temperature dependence of phonon energies along the [001] direction. The energies were measured at 4.7 and 25°K in a sample whose lattice parameter was 4.402 Å (the zero-pressure parameter<sup>2</sup> is 4.463 68 ± 0.000 09 Å). The average temperature shift of the longitudinal mode was found to be positive but small and the average temperature shift of the transverse mode was negative.

Previous first-principles<sup>3</sup> calculations have not accounted for these features although phonon energies within a few percent of the experimental values were obtained with the lowest order self-consistent phonon theory.<sup>4</sup> In this approach the true crystal Hamiltonian is approximated by a model harmonic Hamiltonian whose harmonic-

force-constant matrix  $\Phi$  is determined from the self-consistent condition  $\Phi_{ij} = \langle\langle \nabla_i \nabla_j V \rangle\rangle$ , where the double angular brackets denote the ensemble average calculated with the density matrix appropriate to the model Hamiltonian.

It has been pointed out<sup>4</sup> that contributions from odd-derivative terms should be incorporated into the calculations. Expressions for the leading corrections in a perturbative calculation are similar to those used to obtain anharmonic corrections to the quasiharmonic theory<sup>5</sup> but with ensemble averages of derivatives of the potential substituted for the derivatives evaluated at equilibrium.

Thus, the leading second-order correction (there are no first-order corrections) to the expression given in Ref. 4 for the free energy in lowest order  $F^{(0)}$  is

$$F^{(3)} = -\frac{\lambda^6}{48} \sum_{(1,2,3)} |\langle\langle \nabla_1 \nabla_2 \nabla_3 V \rangle\rangle|^2 \left[ \frac{1+n_1+n_2+n_3+n_1 n_2+n_2 n_3+n_3 n_1}{(\omega_1+\omega_2+\omega_3)} + \frac{3(n_1 n_2+n_1 n_3-n_2 n_3+n_1)}{(\omega_2+\omega_3-\omega_1)} \right] \frac{1}{\omega_1 \omega_2 \omega_3}, \quad (1)$$

and the real  $\Delta$  and imaginary  $\Gamma$  parts of the phonon self-energy are

$$\begin{pmatrix} \Delta_k^{\alpha\beta}(\Omega) \\ \Gamma_k^{\alpha\beta}(\Omega) \end{pmatrix} = -\frac{\gamma^2}{16(\omega_k^\alpha \omega_k^\beta)^{\frac{1}{2}}} \sum_{(1,2)} \langle\langle \nabla_{-k}^\alpha \nabla_1 \nabla_2 V \rangle\rangle \langle\langle \nabla_k^\beta \nabla_{-1} \nabla_{-2} V \rangle\rangle \\ \times \left\{ (n_1+n_2+1) \begin{pmatrix} P(\omega_1+\omega_2+\Omega)^{-1} + P(\omega_1+\omega_2-\Omega)^{-1} \\ \pi\delta(\omega_1+\omega_2+\Omega) - \pi\delta(\omega_1+\omega_2-\Omega) \end{pmatrix} \right. \\ \left. + (n_2-n_1) \begin{pmatrix} P(\omega_1-\omega_2+\Omega)^{-1} + P(\omega_1-\omega_2-\Omega)^{-1} \\ \pi\delta(\omega_1-\omega_2+\Omega) - \pi\delta(\omega_1-\omega_2-\Omega) \end{pmatrix} \right\}. \quad (2)$$

Subscripts denoting wave vectors and superscripts denoting phonon branches have been simplified or eliminated whenever possible in the above expressions. The  $\nabla_k$  notation has been introduced previously.<sup>6</sup> The principal value of  $x^{-1}$  is indicated by  $P(x)^{-1}$ . In preparation for the use of a Lennard-Jones potential, distances are measured in units of  $\sigma$  and energies in units of  $\epsilon$  with  $\lambda^2 = \hbar^2/m\sigma^2\epsilon$ . Temperatures and frequencies will be measured in energy units and  $n_i = [\exp(\beta\omega_i) - 1]^{-1}$  with  $\beta = 1/k_B T$ .

Equations (1) and (2) can be verified in a variety of ways. First of all, they are a limiting form<sup>7</sup> of the more general (but computationally considerably less tractable) second-order expressions of Choquard.<sup>8</sup> Secondly, they can be obtained from an obvious continuation of the work of Horner.<sup>9</sup> Thirdly, as has been pointed out previously<sup>6</sup> and as will be discussed in greater detail in a subsequent publication, one can follow any of the derivations discussed in Ref. 5 with three changes: The potential should be expanded in terms of the eigenfunctions of the self-consistent model Hamiltonian rather than in a Taylor series, the zeroth-order density matrix and phonon states should be appropriate to that Hamiltonian, and terms involving number operators should be eliminated.

In the first work directed at improving the computational power of the self-consistent formalism, Eq. (1) was applied to a study of the thermal properties of solid neon and argon.<sup>10</sup> Space limitations do not permit a discussion of the details, but we would like to emphasize that the results are in considerably better agreement with experiment over the entire temperature range than were previous calculations with less sophisticated theories.

We have meanwhile been studying the implication of Eqs. (1) and (2). Phonon dispersion relations in the [001] direction and the thermal properties of solid neon have been obtained using an all-neighbor model and a Lennard-Jones 12-6 interatomic potential  $V(r) = 4\epsilon[(\sigma/r)^{12} - (\sigma/r)^6]$  whose parameters were chosen to give the experimental lattice spacing and sublimation energy at 0°K in this calculation. The parameters are  $\sigma = 2.7813 \text{ \AA}$  and  $\epsilon = 36.558^\circ\text{K}$ .

The exact method of determining the phonon energies is quite important. The renormalized phonon frequency  $\omega_R$  was not simply identified with  $\omega' = \omega + \Delta(\omega)$ , where  $\omega$  is the lowest order self-consistent phonon frequency, but rather is identified with the maximum of the imaginary part of the Green's function

$$\text{Im}G^{\alpha\alpha} = \text{Im}\left\{ 2\omega^\alpha / [(\omega^\alpha)^2 - \Omega^2 + 2\omega^\alpha \Delta^{\alpha\alpha} - i2\omega^\alpha \Gamma^{\alpha\alpha}] \right\},$$

where  $\alpha = L$  denotes a longitudinal and  $\alpha = T$  a transverse mode.<sup>11</sup> This is the same condition as Eq. (3.4) in Ref. 5 for determining the "best" set of frequencies.

This method is illustrated in Fig. 1 for zone-boundary phonons in the [001] direction. Here,

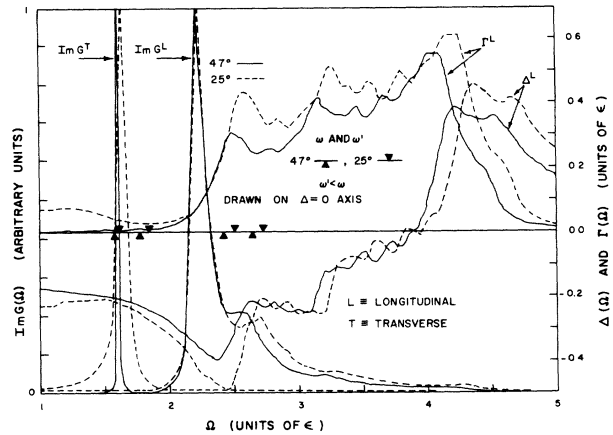


FIG. 1. The imaginary part of the Green's function for longitudinal and transverse zone-boundary phonons in the [001] direction and the real and imaginary parts of the self-energy for the longitudinal mode only as functions of  $\Omega$  at 4.7 and 25°K. The values of the unrenormalized  $\omega$  and incorrectly renormalized  $\omega' \equiv \omega + \Delta(\omega)$  frequencies are also indicated.

$\text{Im}G^{TT}$ ,  $\Delta^{LL}$ , and  $\Gamma^{LL}$  are shown as functions of  $\Omega$  at 4.7 and 25°K. The graph also indicates the position of  $\omega$  and  $\omega'$ .

The most noteworthy features of the graph concern the longitudinal branch and can be readily understood in terms of the behavior of  $\Delta^{LL}$  and  $\Gamma^{LL}$ . The fact that  $\omega_R^L$  differs significantly from  $\omega'^L$  results largely because  $\omega^L$  falls at a local minimum of  $\Delta^{LL}$ ;  $\omega'^L$  then falls in a region where  $\Delta^{LL}$  is larger, giving rise to an even greater shift. The nearly identical shape of  $\text{Im}G^{LL}$  at both temperatures is because  $\omega_R^L(25^\circ\text{K})$  and  $\omega_R^L(4.7^\circ\text{K})$  are nearly equal in value and are located in a region where both  $\Delta^{LL}$  are nearly identical in shape.

Figure 1 also shows that the temperature shift can be different for  $\omega_R$ ,  $\omega'$ , and  $\omega$ . This point is illustrated more fully in Fig. 2, where temperature shifts versus wave vector in the [001] direction are plotted. The agreement with experiment is quite reasonable. Unfortunately, these small effects are very difficult to measure and even the remarkable agreement at the zone boundary does not provide clear evidence for the validity of the calculation.

The experimental and several theoretical phonon dispersion curves in the [001] direction are shown in Fig. 3. The experimental curves were taken from Ref. 1 and were determined there by a force-constant analysis of the neutron-scattering data. The theoretical curves show the phonon energy as determined by the quasiharmonic ap-

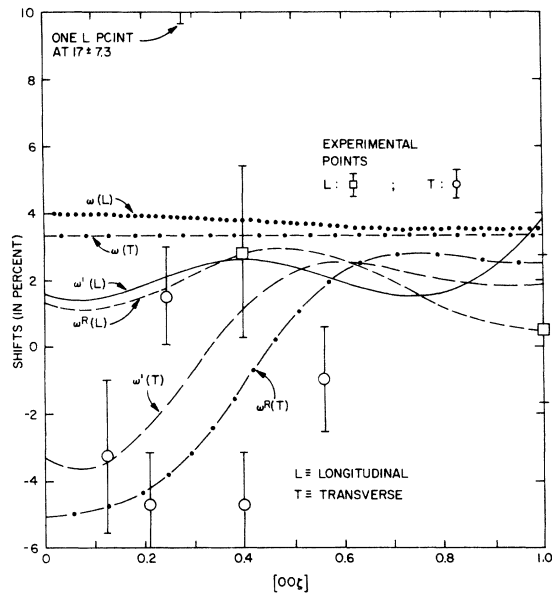


FIG. 2. Temperature shifts, [(higher temperature frequency)–(lower temperature frequency)]/average, between 25 and 4.7°K as functions of wave vector in the [001] direction.

proximation and by  $\omega$ ,  $\omega'$ , and  $\omega_R$  at 4.7°K.

The  $\omega_R$  curves are in fairly good agreement with experiment for the transverse branch and in rather poor agreement for the longitudinal branch. This is probably, in large part, model dependent, a hypothesis which will be tested in future calculations. However, the temperature-shift calculations should be less model dependent.

Striking features of the longitudinal branch are the pronounced flattening of the dispersion curve for  $\omega_R$  near the zone boundary and a quite opposite effect for  $\omega'$ . These effects can easily be explained by the shape of the  $\Delta(\Omega)$  curve in the vicinity of the zone-boundary frequency and by the overall large value of  $\Delta$ . This latter feature is due to the large anharmonicity of solid neon and is probably not model dependent. Since the flattening is not likely to be found by a force-constant analysis of experimental data, a more accurate experimental determination of the longitudinal dispersion curve in the region of the zone boundary would provide an interesting check on a well-defined theoretical prediction.

The sums in  $k$  space were over a bcc grid with 8000 points. The approximations  $P(x)^{-1} \approx x/(x^2 + \eta^2)$  and  $\pi\delta(x) \approx \eta/(x^2 + \eta^2)$  were used, where  $\eta$  was small but finite. The sensitivity of calculations of  $\Gamma$  and  $\Delta$  to the grid size and value of  $\eta$  has been discussed in a recent publication.<sup>12</sup> We have found that  $\omega_R$  is less sensitive to these de-

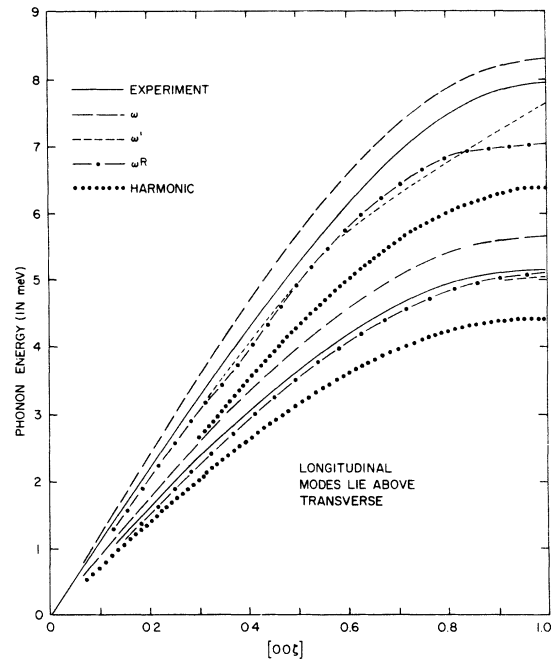


FIG. 3. Experimental and various theoretical phonon dispersion curves in the [001] direction.

tails than is  $\omega'$  provided that the spacing in  $\Omega$  is sufficiently fine. The calculations were performed at 0.01 intervals in  $\Omega$  and  $\eta = 0.05$  was used. Enough numerical experimentation has been performed to indicate that the calculations are reliable. The details will be given later.

The results of our calculations of the thermal properties of solid neon based on an all-neighbor model will be presented in a later publication. They are consistent with those obtained in Ref. 10 with a one-neighbor model. One as-yet-unresolved problem which we intend to investigate is whether any simple two-body potential can be used as the basis for calculations which will successfully predict both the thermal properties and the phonon spectrum of solid neon.

We wish to thank N. R. Werthamer for many valuable discussions and for suggesting plotting the Green's function and J. Skalyo, Jr., for providing the error estimates used in Fig. 2.

<sup>1</sup>J. A. Leake, W. B. Daniels, J. Skalyo, Jr., B. C. Frazer, and G. Shirane, Phys. Rev. (to be published).

<sup>2</sup>D. N. Batchelder, D. L. Losee, and R. O. Simmons, Phys. Rev. **162**, 767 (1967).

<sup>3</sup>That is, a calculation employing no adjustable parameters in which one treats the crystal as a system of atoms which interact through some assumed form of interatomic potential.

<sup>4</sup>N. S. Gillis, N. R. Werthamer, and T. R. Koehler,

Phys. Rev. **165**, 951 (1968). An additional calculation of phonon dispersion curves is plotted in Ref. 1.

<sup>5</sup>R. A. Cowley, Rept. Progr. Phys. **31**, 123 (1968), Pt. 1. References to various derivations can be found here.

<sup>6</sup>T. R. Koehler, Phys. Rev. **165**, 942 (1968).

<sup>7</sup>N. R. Werthamer, unpublished notes.

<sup>8</sup>P. Choquard, *The Anharmonic Crystal* (W. A. Benjamin, Inc., New York, 1967).

<sup>9</sup>H. Horner, Z. Physik **205**, 72 (1967).

<sup>10</sup>V. V. Goldman, G. K. Horton, and M. L. Klein, Phys. Rev. Letters **21**, 1527 (1968), and to be published.

<sup>11</sup>Some notational simplification is used here because  $G$ , which is really a  $3 \times 3$  matrix, is diagonal in the  $[001]$  direction.

<sup>12</sup>L. Bohlin and T. Hogberg, J. Phys. Chem. Solids **29**, 1805 (1968).

## MULTIPLE-PHONON RESONANT RAMAN SCATTERING IN CdS

R. C. C. Leite, J. F. Scott and T. C. Damen

Bell Telephone Laboratories, Holmdel, New Jersey 07733

(Received 15 January 1969)

We have observed  $n$ th order ( $n = 1, 2, \dots, 9$ ) Raman scattering in CdS under conditions of resonance between the laser frequency and the band gap or the associated exciton states. The frequency spectrum of these higher order processes demonstrates that the phonons involved are localized within a small volume of  $k$  space centered at  $\Gamma$ . We believe that such spectral features are characteristic of direct-gap resonant scattering, and the kinematics of their production is discussed.

Different theories of lattice Raman scattering<sup>1-3</sup> have as a common feature terms in the expressions for cross sections which diverge or become very large. This is expressed analytically by the existence of second-order zeroes in the energy denominators of the Raman tensor components. The number of zeroes depends upon the order of the scattering process (i.e., the number of phonons created or annihilated) and upon the kinematic details of the process (such as whether several phonons are produced simultaneously); according to the theory of Birman and Ganguly,<sup>3</sup> for any scattering process which proceeds via electron-photon, electron-lattice interaction, there are at least two such second-order poles present. The first of these poles occurs when the incident photon energy equals the energy of an optical transition in the lattice (e.g., the band gap  $E_g$  or an exciton level  $E_g - R/n^2$ ). In a recent paper<sup>4</sup> we experimentally demonstrated the existence of this pole in CdS for both first- and second-order scattering below the band gap. We showed that the pole was second order and that the resonant state was the first exciton level.<sup>5</sup> The second pole occurs when the scattered-photon energy is equal to that of the optical transition in question. This Letter presents the first experimental evidence for the existence of resonance at the scattered-photon energy. The data consist of intensity measurements of  $n$ th order scattering features ( $n = 1, 2, \dots, 9$ ) in CdS as a function of temperature (hence  $E_g$ ) and laser fre-

quency, for laser frequencies above the band gap. These observations are the first known to the authors of Raman processes higher than fourth.

The data analyzed in the present paper were acquired by reflection scattering from the surface of a single crystal of CdS. An argon laser emitting  $\sim 100$  mW was used as the exciting source and detection was by means of a cooled FW130 photomultiplier, a Keithley 610B electrometer, and a Spex double monochromator. Many geometries were examined, and the results presented here are essentially independent of scattering geometry and were corrected for absorption by means of Loudon's formula.<sup>6</sup>

Figure 1 shows the spectrum obtained from a relatively pure CdS crystal with  $4579\text{-\AA}$  excitation. Significant features of the spectrum are the following: (1) The multiphonon lines are shifted by energies which are approximately 1% less than exact multiples of the first-order LO phonon line at  $\sim 305\text{ cm}^{-1}$ ; (2) these features remain linelike and have widths not much larger than that of the first-order line (e.g.,  $\lambda_2\text{ LO} \approx 1.3\lambda_1\text{ LO}$ ); (3) all processes higher than second disappear when the laser frequency is far below the gap  $E_g/\hbar$ .

We believe that the features observed above may be assigned as due to near zone-center phonons. The evidence for this consists of the following:

(1) Phonon dispersion curves have been calcu-